VOL. 11, NO. 9, MAY 2016 ISSN 1819-6608
ARPN Journal of Engineering and Applied Sciences
©2006-2016 Asian Research Publishing Network (ARPN). All rights reserved.
www.arpnjournals.com

DEVELOPMENTS IN COMPUTER AIDED DIAGNOSIS USED FOR TUBERCULOSIS DETECTION USING CHEST RADIOGRAPHY: A SURVEY

K. G. Satheeshkumar[1] and Alex Noel Joseph Raj[2]
[1]SENSE (School of Electronics Engineering), VIT University, Vellore, Tamil Nadu, India
[2]SENSE (School of Electronics Engineering), Embedded Division, VIT University, Vellore, Tamil Nadu, India
E-Mail: kg.satheeshkumar2013@vit.ac.in

ABSTRACT

One of the major health problems of global concern is Tuberculosis (TB). According to global report of the WHO, approximately 1.3 million people, out of the 8.6 million reported, died of TB in 2012. Most of the TB deaths can be prevented if it is detected at an early stage. Hindrance to this is improper diagnosis at initial stages. Chest X ray (CXR) image is the primary medical diagnosis used for identifying the lung diseases at the first stage. Interpreting the information from CXR depends upon the experience of the physician and the possibility of over and under diagnosis is very high. To identify the disease accurately a proper classification tool along with computer aided diagnosis should be used. Neural network can be used as a classifier tool for the same. Advancement in VLSI technology reduces the computational complexity of Artificial Neural Networks (ANN). Applications of neural networks to medical images (X-ray images of TB and lung cancer) during adolescent stages have resulted in remarkable improvements in diagnosis. This paper describes the fundamentals of radiology of lungs (analysis of CXR), image processing with the aid of ANN and recent developments in this area using computer aided diagnosis (CAD). We have analysed CXR images of several patients and found that an accurate classifier is required for proper diagnosis of TB from these images.

Keywords: Tuberculosis (TB), Computer aided diagnosis (CAD), Chest X Ray (CXR), X-ray imaging, Artificial neural network (ANN).

1. INTRODUCTION

The Bacillus Mycobacterium tuberculosis is the cause of TB among humans. According to the global tuberculosis report of the WHO [1] approximately 1.3 million people died, out of 8.6 million reported with TB, in 2012. Most of TB deaths can be prevented if they are detected at the early stage. According to the WHO, 40% of TB cases are not detected globally. Global Tuberculosis Report 2013 reports that we have to find new measures to eradicate TB to meet the millennium development goals. Case detection is one of the difficulties faced in eradicating this disease. Thorax radiography [2], biological culture [2, 3], Mantoux (tuberculine sensitivity/skin) test [4], interferon-γ tests [5], amplified nucleic acids-based tests [6] (which allow lab-on-chip platforms [7, 8]) and sputum smear microscopy [8, 9] are various methods used to diagnose TB. Among these tests, biological culture and sputum smear microscopy [10] are the most commonly used ones to check whether a subject is contagious. Biological culture is generally accepted as the gold standard, but the test can take up to four weeks [11]. Sputum smear microscopy is typically used to make a decision based on a quick examination. However, smear microscopy has a low sensitivity and is expensive, as an expert microbiologist is needed to diagnose the sputum. CXR imaging is the primary and cheapest medical diagnosis, is widely used for identifying this lung diseases in the initial stage. Interpreting the information from CXR images depends upon the experience of the reader (physician) [12-15] and the possibility of over and under diagnosis is very high. CXR plays a vital role in reducing the delays in diagnosis. Digital CXR imaging helps in storing the image, processing and classifying the abnormalities in the image and has become very accurate and fast. To identify the disease accurately a proper classification tool along with computer aided diagnosis should be used. This can revolutionize case detection even in rural areas by using remote diagnosis with the help of wireless technology.

This paper reviews the applications of ANN technique to CXR imaging to diagnose TB. The rest of the paper is organized as follows; section II discusses the CXR identification case study, section III deals with developments in medical image processing and review of recent research work. The paper concludes with a review of the present status of this subject and an outline of future prospectus in section IV.

2. CHEST X RAY IDENTIFICATION

Posterior-Anterior (PA) and lateral views are the two normally used for CXR (Figure 1a and 1b respectively). Among these the former is the standard view used for diagnosis purpose. All chest X-ray images and medical terms mentioned in this paper are cited in the Chest Atlas [16, 17]. Bone, fluid and air are the three types of densities seen in the CXR (Figure 1c) with white for the first two and black for the air within the lungs. Upper, middle and lower lobes in the right lungs (Figure 1d), and lower lobe and upper lobe along with lingula form the left lung (Figure 1e). Lobes are separated by oblique fissure, and fissure separates between lobes and lingula. Major and minor fissures on lateral chest radiograph are shown in Figures 1f and1g. The inferior portions of

©2006-2016 Asian Research Publishing Network (ARPN). All rights reserved.


Figure 1(a)


Figure 1(b)

Figure 1(c)

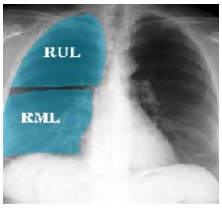

Figure 1(d)

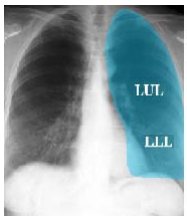

Figure 1(e)


Figure 1(f)

Figure 1(g)

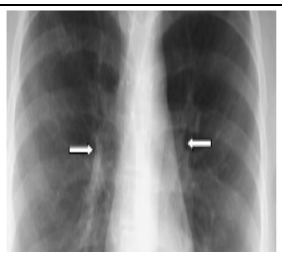
Figure 1(h)

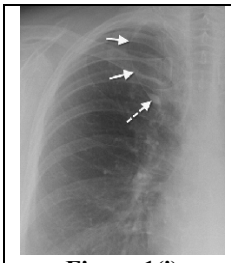
Figure 1(i)

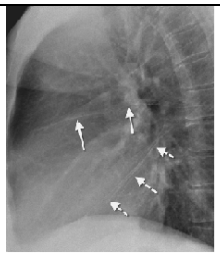
Figure 1(j)


Figure 1(k)


Figure 1(l)

the major fissures and the right minor fissure are shown as dashed white arrows and solid white arrows in Figure 1(i). They outline the location of the right middle lobe. Targeted and magnified view from PA chest radiograph shows the hilar vessels using arrows in Figure 1(h) [18]. The right and left hilar points (where the upper lower veins apparently "cross" the lower lobe artery) are indicated with arrows in Figure 1(j) [18]. The horizontal fissure is seen on a standard PA radiograph as a thin line crossing from the lateral edge of the hemithorax to the hilum. It is very important to identify the surface markings of the lung fissures and the position of the lobes of the lung.

The normally seen abnormalities in CXR may give an indication of TB infiltrate cavity, dense patchy, irregular hazy borders i.e. airspace, cavitary lesion within the lung parenchyma, nodule with poorly defined margins, pleural effusion, enlargement of lymph nodes and linear, interstitial markings. In active pulmonary TB, infiltrates cavities are normally seen along the upper lungs along and fibrotic scars [19] present in the lungs. Slowly multiplying tubercle bacilli develop in nodules and fibrotic scars lead to TB [19]. Persons with above findings should be given treatment at the earliest. Irregularities on chest radiographs are aid for suggesting the chances of TB. Sputum specimens for detailed investigation may be prescribed for persons with above observations. The mentioned standard for bacteriological confirmation of TB is culture based diagnosis in liquid media. It takes more time for getting the results and requires high end laboratories with biosafety infrastructure. Taking standard CXRs is an inexpensive way to screen for the presence of TB but its interpretations are subject to human error and prediction depends on the expertise of the physician [20-22].

The following are some of the examples of CXR to describe the different abnormalities in the chest [23]. The shadow is described as dense homogenous opacity of the right upper zone with the presence of air bronchogram within, indicating that there is a consolidation or solidification of lung (Figure 1k). There is a homogenous opacity in the right lower zone in the PA view, which is seen as a triangular shadow (Figure 1l). Air bronchograms are linear black shadows within a homogenous opacity depicting the air contained in the bronchial tree (Figure-1m), there is a dense homogenous opacity in the lower and outer portion of the left hemi-thorax, with the upper margin slanting toward the axilla suggesting a Pleural Effusion on the Left Side (Figure 1n).

©2006-2016 Asian Research Publishing Network (ARPN). All rights reserved.

Figure 1(m)

Figure 1(n)

Figure 1(o)

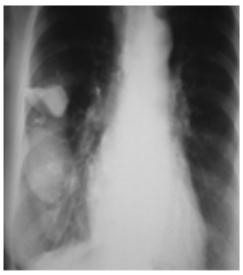

Figure 1(p)

The abnormal amount of fluid development around the lung area is termed pleural effusion; it appears as white space in the base of the lungs. The homogenous opacity (Figure 1o) shown in the right hemi-thorax with an air fluid level is the indication of Hydro-pneumo-thorax.

In Figure 1(p) multiple, rounded or oval shadows and in Figure 1(q) inter-lobar effusion are of the Encysted Pleural Effusions. There is a cavity in the left mid zone with a wall seen on the upper part, an air fluid level in the middle and opacity in the lower part suggesting a Lung Abscess Left Upper Lobe (Figure 1r). There is an area of consolidation with breaking down lesions in the centre, possibly due to TB. The diffuse non homogenous and patchy opacities are suggestive of infiltration due to Tuberculosis (Figure 1s). Multiple small 1-2 mm size mottled opacities are seen on both sides of the lungs more in the mid and lower zones highly suggestive of Miliary Tuberculosis due to a hematogenous spread (Figure 1t).

Figure-1(q)

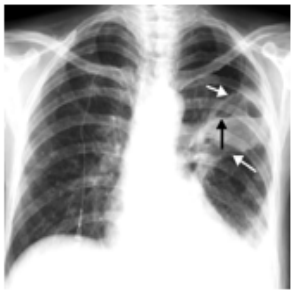

Figure-1(r)

Figure-1(s)

Figure-1(t)

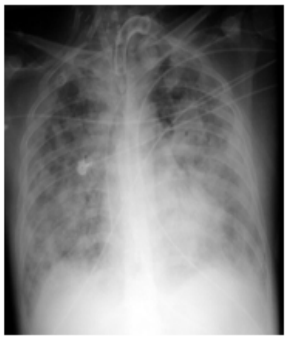

Figure 1(u)

Figure 1(v)

Figure 1(w)

Figure 1(u) is of a patient with acute dyspnoea showing bilateral diffuse non homogenous opacities without air bronchograms suggesting bilateral bronchopneumonia. Figure 1(v) is suggestive of Bilateral Cystic Bronchiectasis, Figure 1(w) showing dense opacity in the hilar region with central hyper-density and peripheral streaking or irregularity is suggestive of Bronchogenic Carcinoma.

The above discussion focuses on the similarities that exist in various abnormalities in the CXR and the possibilities of missed or over-diagnosis of the disease from direct reading of CXR. X-ray images of lung cancer and pulmonary tuberculosis looks similar is an example for this [17]. Hence identifying the abnormality accurately is a challenging issue. To identify the disease accurately, an accurate classification method is required. With the advancements in computing, adequate technology is now available to digitize and store the biomedical images. Once the image data base is available then an efficient classifier program is sufficient for accurate computer aided diagnosis. With the help of computerized image interpretation, inter and intra rate variability by a single or

©2006-2016 Asian Research Publishing Network (ARPN). All rights reserved.

a group of interpreters get reduced. This will improves the confidence level in the patient during a screening study or in a survey [24]. One of the major classifier tools is the neural network technique. ANN finds a lot of applications and that can be used for CXR image classification. The computational complexity of artificial neural network (ANN) is getting reduced with the development of VLSI technologies.

3. DEVELOPMENTS IN MEDICAL IMAGE PROCESSING (TB DIAGNOSIS)

3.1 Artificial Neural Networks (ANN)

ANN is the collection of artificial neurons arranged in some pattern to form a network. With proper training, this network can classify the given inputs according to the training algorithms. The result of this predicts the abnormalities. The idea behind ANN is from the human learning process. ANNs incorporate the two fundamental components of biological neural nets Neurons (nodes) and Synapses (weights). In ANN data is presented to the network in the form of activations in the input layer, passed on to hidden layer and then on to an output layer, data is distributed and processed parallel and if information flow is unidirectional then we call it feed-forward nets. Basic functional diagram of an ANN consisting of input layer, hidden layer and output layer is shown in Figure 2 [25]. Training the network is called learning. As in biological neural learning, in ANN this process taken in an iterative manner by changing the synaptic strength, removing and adding some of the synapses as required by using mathematical optimization techniques. We can train the ANN by using approximation process. To train linear function we need a perceptron and for non linear functions (images), we need a layer of neurons in the network. Bayesian learning and Support vector learning [25] are two types of learning in neural networks. The distribution of the parameters is learnt in the first case, and the minimal representative subset of the available data is used to calculate the synaptic weights of the neurons in the second case. Minimum in a single hidden layer neural network (multi-layer perceptron), radial basis function can be used to learn the approximation of a nonlinear function by changing the output neuron's synaptic weights. For complicated learning, back propagation method is suggested. In this, first we calculate modification values for the synaptic weights of the output side, and then this value is propagated back to (n-1) layers to remove the errors. Alternatives to back propagation are Hebbian learning (Not successful in feed-forward nets), reinforcement learning (Only limited success) and artificial evolution (more general, but can be even slower than back propagation).

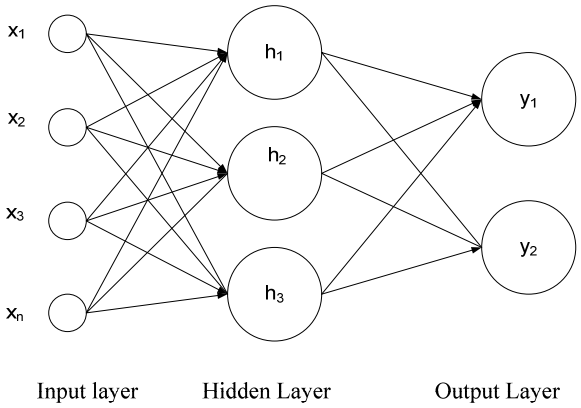

Figure-2. Functional diagram of ANN.

3.2. Image processing

The changes from film based imaging to digitalized radiography have made new development in the TB image screening [26-28]. Digital CXR helps in storing data, processing image and remote transmission of information, more accurate and speedy to classify abnormalities in the image. Opinions from multiple physicians on an image become easy. The open source educational tools like Robochest [29] along with digital CXR can revolutionize case detection even in rural areas by using remote diagnosis with the help of wireless technology.

All images consist of sine and cosine terms, which can be processed with Fourier or Wavelet transforms. Morphological image processing techniques are useful tools for extracting image components such as boundaries and skeletons. Enhancement, noise reduction, segmentation, deblurring, compression, feature extraction and geometric transformations are the basic image processing techniques. Image enhancement is used for sharpening image boundaries so that analysis and graphical display of image will be more precise. In this process the colour manipulation including gray level, noise reduction, filtering, magnification and interpolation are done. The degradation problem can be reduced with filters by image restoration [30]. The number of bits for representing an image can be reduced by image compression. The commonly used format for text, still image and video image compression are CCITT Group 3 and Group 4, JPEG and MPEG respectively. We can perform all image processing operations with Matlab image processing tool box. Thresholding methods (Grey-Level Segmentation), Edge-Detection Techniques, Digital Morphology, Texture and Thinning and Skeletonization algorithms are commonly used in image processing algorithms [31].

The conversion of gray scale image to monochrome image to retrieve the information is used in thresholding or grey-level segmentation. Edge Pixel method, the P-tile method, Iterative method and Fuzzy Sets methods are some other methods to find the threshold. The Edge Pixel method [32] uses a non-directional edge detection operator, Laplacian to form the

©2006-2016 Asian Research Publishing Network (ARPN). All rights reserved.

new histogram by considering pixels having only large Laplacian to compute the threshold values. P-tile method is one of the threshold methods [32] that use the histogram and percentage of black pixels desired by multiplying the percentage by the total number of pixels. By counting the pixels in the histogram bins, starting from 0 bin to bin with the desired number of black pixels, we can find the threshold. The gray level of the last count is considered the threshold. In this method the desired level of black pixels can be changed. The iterative method [32] is a repetition process to calculate the threshold values on the basis of mean gray level values. Initially assumed threshold value is the mean gray level of the image. Then finding the mean gray level of all the pixels below (T_b) and above (T_a) threshold separately and taking the average of them ($(T_b+T_a)/2$) as the new threshold value. This process repeats untill two adjacent iteration processes have the same value and this will be the threshold value. In Fuzzy set method [32], we calculate threshold more accurately by the measure of fuzziness. Here we measure the distance (measure of fuzziness) between the original gray level image and threshold image. If the measurement is a minimum then accuracy is more. The technique used to distinguish the boundary and surroundings of an object is the edge detection techniques, which helps in identifying abnormalities easily. Image filtering and geometric analysis of the structuring elements is done with the use of digital morphology, in which one or other characteristics of the image pixel can be enhanced by using mathematical operations. The repeated patterns in an area are called texture, they may display inconsistency in size, shape and colour. The structural connectivity of the objects is a skeleton. A basic method for skeltonization is thinning i.e. the iterative process in which some of the background points are deleted without affecting the topology of the object. General flow of the image classification with the ANN is shown in Figure-3.

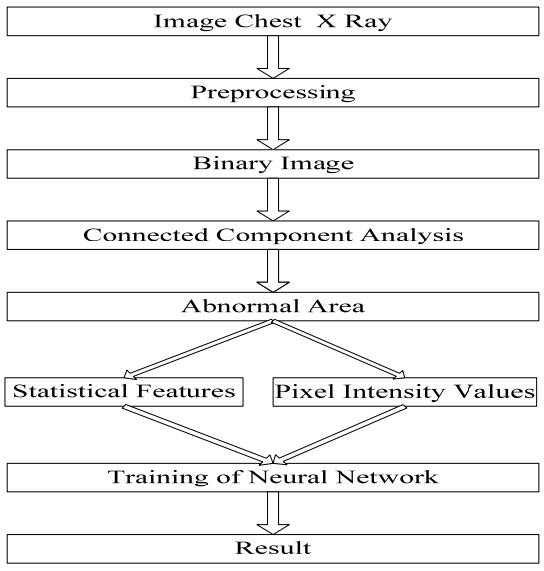

Figure-3. General flow of the image classification with the ANN.

The digitized radiography along with the development of wireless communication has made the diagnosis with the opinion of the multiple physicians or radiologists sitting in different parts of the globe. Good amount of work has been done in the field of image processing. Web based tools for diagnosis of CXR is available in open source educational version [29].

3.3 Computer aided diagnosis

The abnormalities can be identified more precisely by pre and post image processing techniques, assisted by computers which can reduce the errors in the diagnosis. By pre-processing, the nodules, fibrosis, opacities and other abnormalities can become easily visible. Contrast enhancement, lung boundary detection and suppression of bone ribs are a few of the pre-processing steps developed in CAD [33]. Cavity and nodules detection with pattern recognition can be assisted with Bayesian applications [34]. The commonly used technique for the contrast enhancement is histogram equalization, which increases contrast of low contrast regions by spreading the most frequent intensity levels [35]. The wavelet transform and piece-wise linear models used for contrast enhancement are described in cited references [36-38]. One of the bone suppression techniques is described in reference [39], and bone suppressed images can be generated by dual energy imaging techniques [40]. Lung boundaries can be detected by segmentation. The various lung segmentation processes include rule based, pixel classified, deformable models and hybrid model are described in [41]. Thresholding is the key aspect behind the Rule-based algorithm [41] that does not have high accuracy. Pixel classification methods are more accurate with respect to first one as reported in [22], [42], [43] and [44]. Deformable models [45] are more flexible. Active shape models (ASM) [45] and active appearance models (AAM) [46] have been applied to lung boundary detection [47, 48]. By taking advantages of both the above methods a hybrid method has been reported in [49]. Van et al [41, 49] have used internal data sets and the publicly available JSRT [50] data set respectively for this study. The lung boundary detection using ASM and SIFT descriptors [51, 52] on population based and patient specific shape statistics have been studied in descriptors [51, 52], who have reported high segmentation performance. A rule-based method [53] followed by a deformable model approach using low-level features to find the lung boundary has a lower segmentation performance. Jaeger [54] made lung model mask from the training set, for that they have combined intensity model, a lung model mask and log Gabor mask for extracting the lung region. This work has provided them with an accuracy of 83% on their study. Lung mask derived from a training set in combination with a graph-cut algorithm is used to derive lung boundaries by minimizing the graph structure [55].

Lung boundaries are extracted using Kohonen networks [56], a new algorithm proposed for emphysema detection and reported in literature [56]. Lung boundaries are extracted using graph cuts optimization method with

©2006-2016 Asian Research Publishing Network (ARPN). All rights reserved.

energy function, using content-based image retrieval approach for identifying training images, creating the initial patient-specific anatomical model of lung shape using SIFT [57]. Optimization methods using S/T graph cuts for image segmentation are presented in [58]. S/T graph cut is one of the combinatorial optimization methods to extract object on graph based framework; in this S represent source or sink and T represent links of the graph. The authors have suggested a general cost function that includes both region and boundary properties for segmentation. Morphology based segmentation process for lesions are reported in [59]. In that, Segmentation based Partial Volume Analysis (SPVA), a volumetric method which uses region specific histogram to find partial volume effects at the nodule by detecting optimal erosion strength for morphological opening, are addressed. This segmentation method is also used to detect chest wall separation as well as small and large spherical nodules. With respect to the conventional volumetry, SPVA approach increases the volumetric reproducibility, speed and robustness to imaging protocol variations. The milary tuberculosis creates the granular texture to the lung fields has reported in [60]. The milary tuberculosis can be detected using granulometry and correlation with a template matching technique. An algorithm using shape information for segmentation of the lung fields have been developed in [61]. In this the authors have combined the intensity information with shape priors. A fusion of local and global detection methods is presented in [62] where the authors have combined three sub systems for automatic detection of TB from CXR by combining texture and clavicle at pixel level and fused to an image decision and combined with shape decision. This combination technique has improved the performance in detection of TB. 2D Gaussian-model-based template matching for cavity detection and Hessian-matrix-based image enhancement for segmentation and feature extraction with high accuracy and low false positive rate used for automated cavity detection of infectious pulmonary tuberculosis are reported in [63].

Table-1. Various classification methods with reported accuracy

S. No.	Author	Symptoms TB	Classifier	No. of dataset	Accuracy %
1	Noor NM [20]	Pulmonary tuberculosis	PCA	100	94
2	Shen R [34]	Cavity and nodule detection along with pattern recognition	Bayesian	131	82.35
3	Song YL [38]	Focal of pulmonary tuberculosis	Localization algorithm	200	85
4	Tan JH [22]	Pulmonary tuberculosis	Decision tree	95	94.90
5	Ginneken [21]	Lung fields	kNN	248	92
6	Jaeger [54]	Pulmonary tuberculosis	SVM	138	83
7	Sema C [57]	Automatic detection of the lung regions	SIFT	247	95.4
8	Koeslag A[60]	Miliary tuberculosis	Threshold	120	94
9	Xu T [63]	Novel coarse-to-fine dual scale technique for tuberculosis cavity detection in chest radiographs	SVM	35	82.8
10	Arzhaeva [66]	Pulmonary tuberculosis	LDC& voting	42	95
SVM- Support Vector Machine, PCA- Principal Components Analysis, LDC- Linear Discriminator Classifier, kNN- k- Nearest Neighbour, SIFT- Scale Invariant Feature Transform					

Automated methods to segment clavicles in PA CXR by combining multi pixel classification, active shape modelling and dynamic programming to improve the segmentation in clavicles are reported in [64]. A software program to suppress the ribs and clavicles, to remove the noise and equalize the lungs area contrast for detecting lung nodules are explained in [65]. Dissimilarity-based classification method to separate the images of normal and signs of disease is reported in [66]. They have adopted vector classification of the dissimilarity between the prototype and image. The same has been repeated with different prototypes and finally the entire prototypes integrated for classification of the image. Step-wise binary classifiers for the detection of the TB which has reduced the false positives in TB detection from CXR are reported in [67]. Table 1 depicts the various classifiers used with accuracy of the work reported by different researchers. The above discussion gives an overview of the related work in computer aided diagnosis with chest radiography and also shows that there is lot of scope for research in this area.

4. CONCLUSIONS

All the papers cited in this study show that the screening of TB is complex and a proper classification tool needs to emerge. The abnormalities start from subtle milary patterns to effusions. All the surveyed papers describe some of the methods to extract texture and

©2006-2016 Asian Research Publishing Network (ARPN). All rights reserved.

geometry features to classify CXRs into abnormal or normal. Some papers try to address TB detection as a whole while others address only a specific TB manifestation. In this paper we have addressed the various aspects of CXR, image processing basics and ANN for classification. We have carried out a study based on the cited papers for getting an idea to do further research and development on new approaches with more accurate classification of TB and also contribute to Millennium Development Goals (MDGs) as discussed in [1]. This survey can serve as a starting point to give an idea about the need of CAD for TB case detection and provides a brief idea about the image processing and artificial neural network classification methods for future research by identifying new approaches.

REFERENCES

[1] World Health Organization. 2012. Global tuberculosis report. Rep. WHO/HTM/TB/2012.6.

[2] V. Kumar, A. K. Abbas and J. C. Aster. 2012. Robbins Basic Pathology. Philadelphia, PA, USA: Saunders.

[3] R. S.Wallis, M. Pai, D. Menzies, T. M. Doherty, G.Walzl, M. D. Perkins, and A. Zumla. 2010. Biomarkers and diagnostics for tuberculosis: Progress, needs, and translation into practice. Lancet. 375(9729): 1920-1937.

[4] R. Diel, R. Loddenkemper, K. Meywald-Walter, R. Gottschalk, and A. Nienhaus. 2009. Comparative performance of tuberculin skin test,QuantiFERON-TB-Gold in Tube assay, and T-Spot.TB test in contact investigations for tuberculosis. Chest. 135(4): 1010-1018.

[5] A. Zwerling, S. van den Hof, J. Scholten, F. Cobelens, D. Menzies and M. Pai. 2012. Interferon-gamma release assays for tuberculosis screening of healthcare workers: A systematic review.Thorax. 67(1): 62-70.

[6] M. Pai, J. Minion, H. Sohn, A. Zwerling, and M. D. Perkins. 2009. Novel and improved technologies for tuberculosis diagnosis: Progress and challenges Clin. Chest Med. 30(4): 701-716.

[7] C. C. Boehme, P. Nabeta, D. Hillemann, M. P. Nicol, S. Shenai, F. Krapp, J. Allen, R. Tahirli, R. Blakemore, R. Rustomjee, A. Milovic, M. Jones, S. M. O'Brien, D. H. Persing, S. Ruesch-Gerdes, E. Gotuzzo, C. Rodrigues, D. Alland and M. D. Perkins. 2010. Rapid molecular detection of tuberculosis and rifampin resistance. New Engl. J. Med. 363(11): 1005-1015.

[8] D. Boyle and M. Pai. 2012. Tuberculosis: Diagnostic technology landscape.UNITAID Secretariat, World Health Organization, Geneva, Switzerland, Tech. Rep.

[9] K. Steingart, M. Henry, V. Ng, P. Hopewell, A. Ramsay, J. Cunningham, R. Urbanczik, M. Perkins, M. Aziz, and M. Pai. 2006. Fluorescence versus conventional sputum smears microscopy for tuberculosis: A systematic review. Lancet Infect. Dis. 6(9): 570-581.

[10] M. Pai, J. Minion, K. Steingart and A. Ramsay. 2010. New and improved tuberculosis diagnostics: Evidence, policy, practice, and impact.Curr. Opin. Pulmon. Med. 16(3): 271-284.

[11] J. A. Robledo, G. I. Mejia, N. Morcillo, L. Chacon, M. Camacho, J. Luna, J. Zurita, A. Bodon, M.Velasco, J. C. Palomino, A. Martin and F. Portaels. 2006. Evaluation of a rapid culture method for tuberculosis diagnosis: A Latin American multi-center study. Int. J. Tuberc. Lung Dis. 10(6): 613-619.

[12] Nakamura K, Ohmi A, Kurihara T, et al. 1970. Studies on the diagnostic value of 70 mm radiophotograms by mirror camera and the reading ability of physicians. Kekkaku. 45:121-128.

[13] Noor NM, Rijal OM, Yunus A, et al. 2010. A statistical interpretation of the chest radiograph for the detection of pulmonary tuberculosis. In: Biomedical Engineering and Sciences (IECBES), 2010 IEEE EMBS Conference. pp. 47-51.

[14] Schilham AM, van Ginneken B, Loog M. 2006. A computer-aided diagnosis system for detection of lung nodules in chest radiographs with an evaluation on a public database. Med Image Anal 2006.10:247-58.

[15] Toman K, Frieden T. Toman's. 2004. Tuberculosis: case detection, treatment, and monitoring: questions and answers. WHO.

[16] Chandrasekhar A.J. 2006. Chest X-ray Atlas, Select Diseases|Tuberculosis for TB CXR case studies (X-ray pictures showing cavities, infiltrates, scarring, pleural effusion, interstitial nodules of military TB, and TB spine). - from Loyola University Chicago Stritch School of Medicine,http: // www. meddean.luc.edu/ lumen /meded / medicine/ pulmonar/ cxr/atlas/cxratlas_f.htm.

©2006-2016 Asian Research Publishing Network (ARPN). All rights reserved.

[17] Collins, Jannette, Stern, Eric J. 2008. Chest Radiology: The Essentials. 2nd Edition, Lippincott Williams and Wilkins.

[18] Paul Butler, Adam W. M. Mitchell and Harold Ellis. 2007. Applied Radiological Anatomy for Medical Students. Cambridge University Press.pp. 23-27, ISBN-13 978-0-521-81939-8.

[19] Kumar, Vinay; Abbas, Abul K.; Fausto, Nelson; and Mitchell, Richard N. 2007. Robbins Basic Pathology (8th Ed.). Saunders Elsevier. pp. 516-522 ISBN 978-1-4160-2973-1.

[20] Noor NM, Rijal OM, Yunus A, *et al*. 2010. A statistical interpretation of the chest radiograph for the detection of pulmonary tuberculosis. In: Biomedical Engineering and Sciences (IECBES), IEEE EMBS Conference on. pp. 47-51.

[21] Schilham AM, van Ginneken B, Loog M. 2006. A computer-aided diagnosis system for detection of lung nodules in chest radiographs with an evaluation on a public database. Med Image Anal; 10:247-58.

[22] Tan JH, Acharya UR, Tan C, *et al*. 2012. Computer-assisted diagnosis of tuberculosis: a first order statistical approach to chest radiograph.Journal of Medical System. 36:2751-9.

[23] D.Lakshmi, Roy Santhosham, H. Ranganathan. 2013. Comparison of Texture Analysis in the differentiation of Carcinoma from Other Lung Abnormalities Using Low-Dose CT Images', IEEE pp. 978-1-4673-2767-1/13/$31.00, pp. 271-274.

[24] Jones TF, Schaffner W. 2001. Miniature chest radiograph screening for tuberculosis in jails: a cost-effectiveness analysis. Am J Respir. Crit. Care Med 2001; 164: 77-81.

[25] Simon Haykin. 2006. Neural Networks a comprehensive foundation, 2nd edition. PHI chapter 1,p. 29.

[26] Folio L, Stokes R, Frankfurter J. 1995. From film to filmless: military experience with teleradiology in Korea. ApplRadiol. 95:36-39.

[27] Ravin CE, Chotas HG. 1997. Chest radiography. Radiology. 204:593-600.

[28] Summers RM. 2003. Road maps for advancement of radiologic computer-aided detection in the 21st century. Radiology.229:11-13.

[29] Folio LR. 2013. Robochest Web Teaching Tool. Available online: www.robochest.com.

[30] Gonzalez Rafael; Steve Eddins. 2008. Digital Image Processing Using MATLAB (2nd ed.).McGraw Hill. p. 163.

[31] Russ J. C. 1992. The Image Processing Handbook. CRC Press.

[32] Parker J. R 1997. Algorithms for Image Processing and Computer Vision. Wiley Computer Publishing.

[33] McAdams HP, Samei E, Dobbins J 3rd, *et al*. 2006. Recent advances in chest radiography, Radiology. 241:663-683.

[34] Shen R, Cheng I, Basu A. 2010.Hybrid Knowledge-Guided Detection Technique for Screening of Infectious Pulmonary Tuberculosis from Chest Radiographs. IEEE Trans Biomed Eng.

[35] Sherrier RH, Johnson GA. 1987. Regionally adaptive histogram equalization of the chest. IEEE Trans Med Imaging; 6:1-7.

[36] Matozaki T, Tanishita A, Ikeguchi T. 2000. Image enhancement of chest radiography using wavelet transforms. Trans Inst Electron Inf Commun Eng D-II.83:408-414.

[37] Shuyue C, Honghua H, Yanjun Z, et al. 2006. Study of automatic enhancement for chest radiograph. J Digit Imaging.19:371-375.

[38] Song YL. 2010. Localization algorithm and implementation for focal of pulmonary tuberculosis chest image. In: Machine Vision and Human-Machine Interface (MVHI), International Conference on, IEEE.pp. 361-364.

[39] Maduskar P, Hogeweg L, Philipsen R, et al. 2013. Improved texture analysis for automatic detection of tuberculosis (TB) on chest radiographs with bone suppression images. In: SPIE Medical Imaging, pages: 86700H-86700H. International Society for Optics and Photonics.

©2006-2016 Asian Research Publishing Network (ARPN). All rights reserved.

[40] Mac Mahon H, Li F, Engelmann R, et al. 2008. Dual energy subtraction and temporal subtraction chest radiography. Journal of Thoracic Imaging. 23:77-85.

[41] Van Ginneken B, ter Haar Romeny BM, *et al*. 2001. Computer aided diagnosis in chest radiography: a survey. IEEE Trans Med Imaging. 20:1228-41.

[42] Yue Z, Goshtasby A, Ackerman LV. 1995. Automatic detection of rib borders in chest radiographs. IEEE Trans Med Imaging. 14:525-536.

[43] Van Ginneken B, ter Haar Romeny BM. 2000. Automatic segmentation of lung fields in chest radiographs. Med Phys. 27:2445-2455.

[44] Loog M, van Ginneken B. 2006. Segmentation of the posterior ribs in chest radiographs using iterated contextual pixel classification. IEEE Trans Med Imaging. 25: 602-11.

[45] CootesTF, Taylor CJ, Cooper DH, et al. 1996. Active Shape Models-Their Training and Application. Computer Vision Image Understand. 61(1): 38-59.

[46] CootesTF, Edwards GJ, Taylor CJ. 2001. Active appearance models. IEEE Trans Pattern Anal Mach Intell.23:pp. 681-685.

[47] Van Ginneken B, Katsuragawa S, ter Haar Romeny BM,et al. 2002. Automatic detection of abnormalities in chest radiographs using local texture analysis. IEEE Trans Med Imaging.21:139-149.

[48] Van Ginneken B, Frangi AF, Staal JJ, et al. 2002. Active shape model segmentation with optimal features. IEEE Trans Med Imaging.21:924-933.

[49] Van Ginneken B, Stegmann MB, Loog M. 2006. Segmentation of anatomical structures in chest radiographs using supervised methods: a comparative study on a public database. Med Image Anal.10:19-40.

[50] Shiraishi J, Katsuragawa S, Ikezoe J, *et al*. 2000. Development of a digital image database for chest radiographs with and without a lung nodule: receiver operating characteristic analysis of Radiologist's detection of pulmonary nodules', AJR Am J Roentgenol.174:71-74.

[51] Shi Y, Qi F, Xue Z, *et al*. 2008. Segmenting lung fields in serial chest radiographs using both population-based and patient-specific shape statistics. IEEE Trans Med Imaging.27:481-94.

[52] Shi Y, Shen D. 2008. Hierarchical shape statistical model for segmentation of lung fields in chest radiographs. Med Image ComputComput Assist Interv.11:417-424.

[53] Annangi P, Thiruvenkadam S, Raja A, *et al*. 2012. A region based active contour method for x-ray lung segmentation using prior shape and low level features. Biomedical Imaging: From Nano to Macro2010, IEEE International Symposium2012. pp. 892-5.

[54] Jaeger S, Karargyris A, Antani S, *et al*. 2012. Detecting tuberculosis in radiographs using combined lung masks. Conference Proceedings IEEE Eng. Med BiolSoc 2012. pp. 4978-4981.

[55] Candemir S, Jaeger S, Palaniappan K, et al. 2012.Graphcut based automatic lung boundary detection in chest radiographs. In: First IEEE Healthcare Technology Conference: Translational Engineering in Health and Medicine, Houston, USA, 2012:pp. 31-34.

[56] Coppini G, Miniati M, Monti S, *et al*. 2013. A computer-aided diagnosis approach for emphysema recognition in chest radiography. Med Eng. Phys.35:pp. 63-73.

[57] SemaCandemir, Stefan Jaeger *etal*. 2013. Lung Segmentation in Chest Radiographs Using Anatomical Atlases with Non-rigid Registration.DOI 10.1109/TMI.2013.2290491, IEEE Transactions on Medical Imaging. 10(10).

[58] Yuri Boykov, Gareth Funka-Lea. 2006. Graph Cuts and Efficient N-D Image Segmentation, International Journal of Computer Vision. 70(2): 109-131, Springer Science + Business Media, LLC. Manufactured in The Netherlands. DOI: 10.1007/s11263-006-7934-5.

[59] Jan-Martin Kuhnigk, Volker Dicken, Lars Bornemann, Annemarie Bakai, Dag Wormanns, Stefan Krass, and Heinz-Otto Peitgen. 2006. Morphological Segmentation and Partial Volume Analysis for Volumetry of Solid pulmonary Lesions in Thoracic CT Scans. IEEE Transactions on Medical Imaging. 25(4): 417-434.

[60] Koeslag A, de Jager G. 2001. Computer aided diagnosis of miliary tuberculosis. Proceedings of the Pattern Recognition Association of South Africa.

©2006-2016 Asian Research Publishing Network (ARPN). All rights reserved.

[61] A. Dawoud. 2010. Fusing shape information in lung segmentation in chest radiographs. Image Analysis and Recognition. pp. 70-78.

[62] L. Hogeweg, C. Mol, P. de Jong, R. Dawson, H. Ayles and B. van Ginneken. 2010. Fusion of local and global detection systems to detect tuberculosis in chest radiographs.In Medical Image Computing and Computer-Assisted Intervention (MICCAI). pp. 650-657.

[63] T. Xu, I. Cheng and M. Mandal. 2011. Automated cavity detection of infectious pulmonary tuberculosis in chest radiographs. In: Int. Conf. IEEE Engineering in Medicine and Biology Society (EMBS). pp. 5178-5181.

[64] L. Hogeweg, C. I. S´anchez, P. A. de Jong, P.Maduskarand B. van Ginneken. 2012. Clavicle segmentation in chest radiographs. Medical Image Analysis. 16(8): 1490-1502.

[65] M. Freedman, S. Lo, J. Seibel and C. Bromley. 2011. Lung nodules: Improved detection with software that suppresses the rib and clavicle on chest radiographs. Radiology. 260(1): 265-273.

[66] Y. Arzhaeva, D. Tax and B. Van Ginneken. 2009. Dissimilarity-based classification in the absence of local ground truth: Application to the diagnostic interpretation of chest radiographs. Pattern Recognition. 42(9): 1768-1776.

[67] C. Pangilinan, A. Divekar, G. Coetzee, D. Clark, B. Fourie, F. Lure and S. Kennedy. 2011. Application of stepwise binary decision classification for reduction of false positives in tuberculosis detection from smeared slides. In Imaging and Signal Processing in Healthcare and Technology.